CI&CEQ
Chemical Industry & Chemical Engineering Quarterly

Available online at
Association of the Chemical Engineers of Serbia AChE
www.ache.org.rs/CICEQ
Chem. Ind. Chem. Eng. Q. 33 (1) xxx–xxx (2027) CI&CEQ

MAJA DJEPANOVA
https://orcid.org/0009-0008-0251-3906
BILJANA STEFANOVSKA
https://orcid.org/0009-0002-2937-7760
ANGELA NASTEVSKA
https://orcid.org/0009-0000-3169-3194
TEODORA TASEVSKA
https://orcid.org/0009-0002-9615-8322
LINA LIVRINSKA TRPEVSKA
https://orcid.org/0009-0007-7569-4448
KATERINA GORACINOVA
https://orcid.org/0000-0002-8101-6359
NIKOLA GESKOVSKI
https://orcid.org/0000-0002-2073-5632
MAJA SIMONOSKA CRCAREVSKA
https://orcid.org/0000-0002-1927-7101

Faculty of Pharmacy, Ss. Cyril & Methodius University in Skopje, Republic of North Macedonia

EXPLORATORY QUALITY BY DESIGN STUDY OF LIDOCAINE HYDROCHLORIDE EMULGELS

Highlights

- QbD-guided formulation development defined LHCl emulgel structure-function relationships
- Excipient ratio governed droplet size and viscoelastic network structure
- Carbopol and Cetostearyl alcohol increased yield stress and elastic dominance
- Isopropyl myristate and Tween 80 reduced matrix rigidity and accelerated release
- Gel network strength at 32 °C correlated to dissolution behavior

Abstract

A quality by design/quality risk management-driven early-stage screening was conducted for 4% lidocaine hydrochloride (LHCl) oil-in-water emulgels intended for topical use. A quality target product profile was established and critical quality attributes defined to ensure efficacy, safety, and patient acceptability. Nine formulations (B1-B9) were developed to evaluate the influence of key critical material attributes, Carbopol 940, Tween 80, cetostearyl alcohol (CA), and isopropyl myristate (IPM), on physicochemical properties, rheology, spreadability, and in vitro drug release. All formulations showed acceptable pH, homogeneity, and drug content. Droplet size and polydispersity depended strongly on excipient composition: higher Carbopol and CA increased droplet size, whereas Tween 80 reduced it. Amplitude sweep measurements demonstrated elastic-dominant behavior within the linear viscoelastic region; Carbopol and CA enhanced viscoelastic strength and yield stress, while Tween 80 and IPM exhibited a plasticizing effect. Spreadability was comparable across formulations and reflected shear-thinning behavior. In vitro dissolution revealed formulation-dependent LHCl release, with stronger gel networks associated with slower release. Correlation analysis confirmed significant relationships between CA content, rheological parameters, droplet size, and drug release. Overall, LHCl emulgels can be rationally designed using a quality by design (QbD) approach, with rheology and droplet size serving as key determinants of performance.

Keywords: quality by design, quality risk management, topical drug delivery, emulgel formulation.

SCIENTIFIC PAPER

UDC

INTRODUCTION

Emulgels represent a hybrid topical drug delivery platform in which an emulsion, either oil-in-water (O/W) or water-in-oil (W/O), is immobilized within a three-dimensional gel matrix. By combining the structural and functional advantages of both emulsions and gels, emulgels act as dual controlled-release systems capable of enhancing drug residence time on the skin and improving permeation. In emulsions, the internal phase serves as a reservoir from which the drug slowly migrates into the external phase and subsequently across the skin barrier. Incorporation of the emulsion into a gel base further strengthens this effect by creating a pseudoplastic system that spreads easily, resists runoff, and maintains prolonged contact with the application site. Gelling polymers also modulate viscosity, enhance stability, and influence drug release kinetics, while surfactants and oils can function as permeation enhancers. Despite some formulation challenges such as potential air entrapment and limitations in delivering macromolecules, emulgels are widely regarded as elegant, non-greasy, washable, and highly acceptable dosage forms to patients [1].

Correspondence: M. Simonoska Crcarevska, Faculty of Pharmacy, Ss. Cyril & Methodius University in Skopje, Majka Tereza 47, 1000 Skopje, Republic of North Macedonia.
Email: msimonoska@ff.ukim.edu.mk
Paper received: 3 March 2026
Paper revised: 13 June 2026
Paper accepted: 5 July 2026

https://doi.org/10.2298/CICEQ260303008D

Compared with low-viscosity aqueous gels or microemulsions, emulgels provide better retention on the skin surface, allowing extended contact time that facilitates drug diffusion through the stratum corneum. Lipid components and surfactants such as these can improve drug partitioning into the lipid-rich outer layers of the epidermis. These properties are particularly valuable for topical anesthetics, where enhanced permeation may shorten onset time and prolong duration of action. Recent studies have demonstrated that emulsion-based gels containing local anesthetics can achieve improved therapeutic performance due to the synergy between emulsion microstructure and gel-mediated rheological behavior [2].

Topical delivery systems in general offer significant advantages over oral and injectable routes, which frequently suffer from low bioavailability, delayed onset, and systemic adverse effects. Skin-based delivery enables targeted administration directly to the site of action while minimizing systemic exposure. Not only are topical systems foundational in dermatology, but they are increasingly employed for procedures in aesthetic medicine, minor surgery, and pain management, where rapid and localized anesthetic effect is desired [3].

Lidocaine hydrochloride (LHCl) is a widely used local anesthetic valued for its rapid onset of action and favorable safety profile. In addition to its established use in dermatology, dentistry, minor surgery, and emergency medicine, lidocaine is routinely applied for both acute and chronic pain management, as well as in aesthetic procedures requiring short-term surface anesthesia [4].

Emulgels represent a promising platform for LHCl because their biphasic structure enhances drug partitioning into the skin while maintaining desirable rheology, spreadability, and non-greasy application properties. Despite lidocaine's extensive clinical usage, there is comparatively limited research specifically examining LHCl incorporated into emulgel matrices [5].

The selection of an emulgel platform over a conventional aqueous gel was based on its ability to combine a hydrated polymeric network with an internal lipid phase. This architecture is expected to enhance residence time at the application site, facilitate drug partitioning into the lipid-rich stratum corneum, and provide more controlled drug release while maintaining the desirable properties of a non-greasy, washable semisolid dosage form [1,2]. For LHCl, which is highly water-soluble yet must permeate beyond the outer skin barrier to exert its anesthetic effect, the coexistence of aqueous, lipid, surfactant, and gel domains may enable more controlled drug release and skin permeation compared with a conventional gel matrix. In such systems, macroviscosity can modulate the diffusion of dispersed droplets, while microviscosity influences molecular diffusion within the vehicle, thereby affecting overall release behavior [6].

The aim of this study was to apply a quality by design (QbD) framework to explore composition-performance relationships of 4% lidocaine HCl emulgels and to prioritize critical material attributes (CMAs) and critical process parameters (CPPs) for subsequent DoE using a QRM (FMEA) approach. The influence of the gelling agent, surfactant level, and oil phase was screened in relation to physicochemical attributes, including droplet size, polydispersity index, pH, drug content, and in vitro dissolution behavior. Rheological behavior and spreadability were evaluated as supportive, formulation-ranking tools to gain indicative insight into structural organization and application performance.

MATERIALS AND METHODS

Materials

Lidocaine hydrochloride (LHCl) (Moehs, Spain) was kindly donated by Alkaloid AD Skopje, North Macedonia, and used as the active pharmaceutical ingredient. Carbopol (Sigma-Aldrich, Germany) served as the gelling agent, while distilled water was used as the aqueous phase. Polysorbate 80 (Tween 80) (Merck, Germany) and sorbitan monooleate (Span 80) (Merck, Germany) acted as non-ionic emulsifiers, and cetostearyl alcohol (CA) (Merck, Germany) functioned as a co-emulsifier and viscosity enhancer. Isopropyl myristate (IPM) (Basf, Germany) was included as a penetration enhancer and oil-phase component. Methylparaben and propylparaben (Fluka Analytical, Japan) were used as preservatives. Propylene glycol (Fischer Scientific, Netherlands) served as a co-solvent and humectant, while triethanolamine (TEA) (Alkaloid AD Skopje, North Macedonia) was used for pH adjustment and carbopol neutralization.

Methods

QbD Approach

The development of the 4% LHCl emulgel followed the QbD principles outlined in ICH Q8(R2) [7]. The quality target product profile (QTPP) for a dermal semisolid was defined, followed by identification of critical quality attributes (CQAs) relevant to product performance and patient safety. Critical material attributes (CMAs) and critical process parameters (CPPs) were determined by assessing formulation components and processing steps with potential impact on these CQAs. Risk assessment was performed using Failure Mode and Effects Analysis (FMEA) to prioritize variables requiring control.

Formulation Preparation

Preliminary one-factor-at-a-time (OFAT) trials were conducted to support process understanding and to outline the initial design space for robust emulgel formulation.

Nine 4% LHCl emulgel formulations (B1–B9) were prepared, with Table 1 listing only the components that varied among formulations; all other ingredients were kept constant. In a clean 100 mL glass vessel, 4 g of LHCl were accurately weighed and dissolved in the first portion of purified water (50 g). Subsequently, carbopol was added and dispersed at 40 ± 2 °C using a magnetic hotplate stirrer with temperature controller (IKA Plate (RCT Digital), IKA Werke, Germany) set at 300 rpm until a clear, colorless colloid was formed. In a separate 100 mL vessel, the oil phase composed of CA, IPM, as well as Tween 80, and Span 80 (0.75 g) was stirred for 4-5 min using a magnetic stirrer (IKA Plate (RCT Digital), IKA Werke, Germany) at

300 rpm and heated to 70 ± 2 °C until complete liquefaction of the oil phase was achieved. The oil phase was gradually incorporated into the aqueous phase by dropwise addition, using high-shear homogenization (Ultra Turrax homogenizer T25 basic, IKA-WERKE, Germany) at 6000 rpm for 20–25 min at 40 °C. After formation of the emulsion and cooling to room temperature (without stirring), TEA was added dropwise under continuous manual stirring to adjust the pH to 5.0–7.0, thereby inducing carbopol neutralization and gel formation. Subsequently, propylene glycol (7.5 g), in which the preservatives, methylparaben (0.2 g) and propylparaben (0.1 g) had been previously dissolved, was incorporated into the emulgel matrix, followed by the gradual addition of the remaining quantity of purified water (to a final mass of 100 g). The resulting formulation was manually mixed for an additional 15 min to ensure homogeneity of the emulgel.

Table 1. Composition of the 4% LHCl emulgel formulations showing only components that varied among formulations

Sample	Carbopol	Tween 80	Cetostearyl Alcohol	Isopropyl Myristate
B1	0.5	1	2	5
B2	0.75	1	2	5
B3	1	1	2	5
B4	0.5	1.5	2	5
B5	0.5	2	2	5
B6	0.5	1	3.5	5
B7	0.5	1	5	5
B8	0.5	1	2	7.5
B9	0.5	1	2	10

pH measurement

The pH of each emulgel formulation was determined using a calibrated benchtop pH meter (Biobase PHS-3BW, China). Prior to analysis, the instrument was calibrated using standard buffer solutions at pH 4.0, 7.0, and 9.0. pH measurements were performed directly on the emulgel samples at 25 ± 2 °C. Each formulation was analyzed in triplicate, and results are reported as mean ± standard deviation (SD).

Droplet size and polydispersity index

The droplet size (DS) and polydispersity index (PDI) of the emulgel formulations were determined using a Zetasizer Nano ZS (Malvern Instruments, UK).

For droplet size analysis, the samples were sufficiently diluted to ensure translucency; approximately 0.5 g of emulgel was diluted in 10 mL of deionized water and gently mixed manually to obtain a uniform dispersion without disrupting the emulsion droplets. Aliquots of each emulgel formulation were placed in disposable folded capillary cells, and measurements were performed after a temperature equilibration period of 120 s. The dispersing medium had a viscosity of 0.8894 cP, a dielectric constant of 78.5, and measurements were conducted at a scattering angle of 173° at 25 °C. Each sample was measured in triplicate, with each measurement consisting of multiple automatically optimized sub-runs to ensure accuracy and reproducibility. Data are presented as the mean ± SD.

Rheological properties

Nine 4% LHCl emulgel formulations (B1–B9) were characterized using a modular compact rheometer equipped with a Peltier temperature control device (MCR 92, Anton Paar Rheometer, Austria). The storage modulus (G'), loss modulus (G''), loss factor (tan δ), torque, and complex viscosity (η^*) were measured using an amplitude sweep method, based on the procedure described by Dutta *et al.* [8] with slight modifications. The measurements were performed on 1 mL of each formulation using a cone (CP50-1) geometry, with the zero gap set to 0.104 mm and a 30 s equilibration period prior to testing. The analyses were conducted at 25 ± 0.2 °C and 32 ± 0.2 °C, with an angular frequency of 10 s^{-1} and a shear strain range from 0.1 to 1000%. During each 500-second measurement, 21 data points were recorded. Rheological measurements were performed in duplicate for each formulation at the temperature and were intended as a preliminary screening assessment of viscoelastic behavior and structural stability rather than as definitive quantitative characterization.

The linear viscoelastic region (LVR) of each formulation was determined from the strain-dependent behavior of the storage modulus. The plateau storage modulus (G'_0) was calculated as the mean of the first five data points at the lowest shear strains, representing the range where the material exhibits predominantly elastic behavior. The LVR limit strain (γ_{LVR}) [9,10] was then defined as the shear strain range over which G' remained approximately constant, with deviations not exceeding 5% of G'_0 [11]. Within this region, mean values of the storage modulus (G'_{LVR}), loss modulus (G''_{LVR}), and loss factor (tan δ_{LVR}) were calculated. The shear stress at the LVR limit strain (γ_{LVR}) was taken as the yield stress (τ_{yield}). The LVR viscosity (η_{LVR}) was calculated as the average of the complex viscosities within the LVR. Additionally, the complex viscosity at the yield point (η_{yield}) was determined, while minimum and maximum torque values were extracted from the full amplitude sweep.

Data processing and calculation of rheological parameters were performed using Python (version 3.12.2) with Pandas and NumPy libraries. All calculations, including identification of the LVR and derivation of rheological parameters, were automated to ensure reproducibility and consistent treatment. The compiled summary tables for each formulation and storage condition were subsequently used for comparative evaluation of structural properties and correlation with physicochemical characteristics and drug release performance.

Spreadability

The spreading capacity of the emulgel formulations was evaluated using the parallel plate method [12]. Briefly, 0.5 g of emulgel was placed dropwise at the center of a clean glass plate, and a second glass plate with a standardized weight of 0.49 N (49.979 g) was placed on top. The diameter of the spreading gel was recorded at intervals of 5 s from 0 to 60 s, 10 s from 70 to 120 s, and 60 s from 180 to 600 s, using a graph paper scale.

The percentage of spreadability was calculated as:

$$\%\text{Spread} = \frac{D_n}{D_1} \times 100 \quad (1)$$

where D_1 is the initial gel diameter and D_n is the diameter at each measured time point.

Spreadability measurements were conducted on a single batch per formulation, serving as a preliminary screening tool to assess relative spreading behavior and topical applicability. As only one batch was tested, and given the exploratory nature of the study, results were interpreted descriptively rather than quantitatively.

Drug content assay

Approximately 0.6 g of emulgel was accurately weighed and quantitatively transferred into a 25 mL volumetric flask. Around 70% of the final volume of the extraction solvent, a 1:1 (v/v) mixture of acetonitrile and 0.1% (v/v) phosphoric acid in water, was added, and the sample was vortex-mixed for 5 min, followed by sonication in an ultrasonic bath (Ultrawave U300, UK) for 15 min. Afterwards, the flask was filled to volume with the same solvent and mixed thoroughly to ensure homogeneity. An aliquot of 1.0 mL of the resulting solution was further diluted to 5.0 mL with the same extraction solvent. Prior to analysis, the sample was filtered through 0.45 µm regenerated cellulose membrane filters (Sartorius, Germany).

Chromatographic separation [13] was performed using an Agilent HPLC system (1100) equipped with a C18 reversed-phase column (Eclipse XDB 150 × 4.6 mm, 5 µm particle size, Agilent). The mobile phase consisted of solvent A (0.1% v/v phosphoric acid in water) and solvent B (acetonitrile), and the analysis was carried out using a gradient elution program: 0 min – 10% B, 10 min – 90% B, 15 min – 10% B, maintained at 10% B until 20 min for reequilibration. The flow rate was 0.8 mL/min, the column temperature was maintained at 25 °C, and the injection volume was 5 µL. Detection was performed at 210 nm using a UV-Vis detector. A calibration curve for the analyte was constructed using standard solutions over 120 - 400 µg/ml concentration, and the linearity was confirmed by the correlation coefficient ($R^2 \geq 0.99$) and by the closeness of the y-intercepts to zero. The limit of detection and limit of quantification were determined based on the calibration curve approach in accordance with ICH guidelines Q2(R2) [14]. The Standard Deviation of the response (σ) was taken as the standard error of the intercept, and the slope (S) was obtained from linear regression analysis.

In vitro drug release

The in vitro release of LHCl from the emulgel formulations was evaluated using a membrane diffusion method. Donor and receptor chambers were separated by a dialysis membrane (MEMBRACEL®, regenerated cellulose, MWCO 7000 Da, Serva, Germany) with a diffusion area of 1.23 cm^2.

Release studies were performed in triplicate using deionized water, adjusted to pH 5.5 ± 0.2 with phosphoric acid, as the receptor medium. The experiments were carried out under sink conditions at 32 ± 0.5 °C in a shaking water bath (Haaken, type SWB20, Germany). The donor compartment contained 2 g of the emulgel formulation or an equivalent aqueous LHCl solution as a reference standard. When fully released into the 40 mL dissolution medium, this amount corresponds to a theoretical LHCl concentration of 2 mg/mL, ensuring sink conditions. The receptor medium was continuously agitated at 50 rpm.

At predetermined time intervals (0.5, 1, 2, 3, 4, 5, 6, and 24 h), 5 mL aliquots were withdrawn from the receptor compartment and immediately replaced with an equal volume of pre-equilibrated receptor medium to maintain sink conditions. The concentration of LHCl in collected samples was quantified using the validated HPLC method described in the assay section. Data are expressed as mean ± SD (n=3).

Similarity between dissolution profiles was evaluated using the similarity factor (f_2). Pairwise comparisons were conducted to assess the similarity of dissolution profiles between formulations with systematic variation of formulation components. Dissolution profiles were considered similar when f_2 values were ≥ 50. Mean dissolution time (MDT) was calculated from the cumulative dissolution data as a model-independent parameter to further characterize release behavior. The MDT and f_2 calculations were performed using DDSolver 1, a menu-driven add-in program for Microsoft Excel [15].

Correlation analysis and visualization

Correlation analysis and visualization were performed using Python (version 3.12) (pandas, seaborn, and matplotlib libraries). Rheological, physicochemical, and dissolution parameters were analyzed for each formulation (B1-B9). Correlation matrices were calculated using Pearson's correlation coefficient (r) across all measured formulation parameters.

Separate correlation matrices were generated for parameters measured at 25 °C, including rheological and physicochemical variables, and 32 °C, including rheological, physicochemical properties, and dissolution-related parameters.

Correlation matrices were visualized as heatmaps, with correlation coefficients displayed directly within each cell. A diverging color scale centered at zero was used to distinguish positive and negative correlations, facilitating rapid visual identification of strong associations between formulation attributes. All correlation matrices were exported as CSV files and chart plots to ensure transparency and reproducibility of the analysis.

RESULTS

Quality Target Product Profile (QTPP)

The QTPP for the 4% LHCl emulgel is summarized in Table S1. The formulation was designed as an oil-in-water (O/W) topical emulgel, combining the enhanced skin permeation of an emulsion with the spreadability and residence time of a gel. It was intended for topical application, providing local anesthesia while minimizing systemic exposure, with a dosage strength of 4% LHCl (40 mg/g). Physical attributes were defined to ensure a smooth, homogeneous, white/off-white semisolid without phase separation, indicating proper emulsification and

gelation. Key quality attributes included pH (5.0–7.0), pseudoplastic viscosity within predefined limits, reproducible spreadability, drug content within 90–110% of the label claim, content uniformity compliant with Ph. Eur. [16] standards, and a controlled drug release profile. Microbiological quality should conform to Ph. Eur. 5.1.4 [16], and preservative efficacy should meet Category A requirements. The formulation was designed for stability of at least 24 months under ICH long-term conditions, maintaining chemical, physical, and microbiological integrity. Packaging in light-protective, airtight containers was specified to preserve product quality, with container sizes of 15–50 g for practical use. No alternative administration routes were intended, as the formulation specifically supports dermal application and local anesthetic effect.

Critical Quality Attributes (CQAs)

The CQAs (Table S2) were defined to ensure product efficacy, safety, and patient acceptability. Key CQAs included pH (5.0–7.0), viscosity (pseudoplastic flow), and spreadability (uniform spread diameter of ≥4 cm), which directly influence skin compatibility, residence time, and controlled drug release. Drug content (90–110% of label claim) and content uniformity (RSD ≤ 5% per Ph. Eur. [16]) were critical for ensuring accurate dosing and predictable therapeutic effect. The drug release profile was designed to achieve controlled release, affecting both onset and duration of anesthesia. Microbiological quality and preservative efficacy were also identified as CQAs due to their impact on safety; however, they are largely governed by raw material quality and controlled manufacturing conditions, and are not expected to be directly affected by formulation or process variations. Together, these CQAs define the formulation parameters critical for maintaining consistent product performance, safety, and patient acceptability.

Quality risk management (QRM)

A QRM assessment was conducted using an FMEA approach (Tables S3 and S4). This assessment considered both CMAs and CPPs and their potential impact on product quality, safety, and efficacy.

Among the CMAs, Carbopol 940 exhibited the highest risk, with deviations in hydration or concentration potentially affecting viscosity, gel network formation, and drug release (RPN = 24). Emulsifiers, including Span 80, Tween 80, and CA, were assigned a moderate risk level (RPN = 18) based on their known influence on emulsification, phase stability, and droplet size as reported in previous studies and formulation experience. In contrast, LHCl, TEA, preservatives, and the oil-water ratio were considered to have lower risk levels (RPN < 10) under the applied formulation and processing conditions. It should be noted that, while the OFAT experiments provided experimental insight into selected CMAs and CPPs, certain parameters such as TEA and the oil-water ratio were assessed primarily based on prior knowledge. Future refinement of the initial risk assessment may include targeted OFAT studies for these critical parameters to experimentally verify their impact on CQAs, particularly given the sensitivity of Carbopol 940 to pH changes and ionic strength.

CPPs previously optimized in preliminary experiments, including mixing speed, emulsification temperature, cooling rate, and mixing time, were assigned low RPN values (<10), indicating limited potential to negatively affect CQAs when controlled within defined operational ranges.

The initial risk assessment (Table S4) highlighted that drug content, content uniformity, and drug release profile are most sensitive to variations in CMA, particularly Carbopol 940 and emulsifiers, whereas microbiological quality and preservative efficacy, as was already noted, are largely influenced by raw material quality and controlled manufacturing environments rather than formulation and process parameter variations. Other CQAs, such as pH, viscosity, and spreadability, indicate variable sensitivity to different CMAs, with TEA identified as a moderate contributor to pH variability.

Overall, the QRM process allowed identification and prioritization of high- and moderate-risk material attributes and process parameters, guiding the focus for further development, control strategy design, and experimental verification to ensure consistent product quality, efficacy, and safety.

Preparation of LHCl emulgel

Nine LHCl (4%) emulgel formulations (B1-B9) were successfully prepared with total batch weights of 100 g. Formulations B1-B9 were grouped to assess the effect of specific CMAs on critical quality attributes. Formulations B1-B3 were used to evaluate the impact of Carbopol concentration on gel rheology, spreadability, and drug release. The influence of Tween 80 on emulsification efficiency and phase stability was investigated using formulations B1, B4, and B5. The role of CA in modulating emulgel consistency and droplet stability was assessed using formulations B1, B6, and B7. Finally, variations in IPM were explored across formulations B1, B8, and B9.

All batches were prepared by first forming the aqueous phase, dissolving Carbopol and LHCl in water, followed by emulsification with the heated oil phase containing surfactants, CA, and IPM. High-shear homogenization ensured uniform droplet size and emulsion consistency. Neutralization with TEA induced gelation, and propylene glycol and preservatives were incorporated at the final stage. All formulations produced smooth, homogeneous, white/off-white semisolids without visible phase separation or particulate matter, suitable for further characterization.

pH measurement

Measured pH values of the formulations at initial testing and during hold-time stability are presented in Table 2. pH values ranged from 5.82 to 6.68. All measured pH values for all samples remained within the predefined acceptable limits for topical semisolid formulations (5.0–7.0).

Table 2. pH values, droplet size, and polydispersity index values of the formulations (n=3).

Formulation	pH ±SD	Droplet size (nm ± SD)	PDI±SD
B1	6.41 ± 0.04	289.4 ± 5.0	0.542 ± 0.023
B2	6.29 ± 0.01	300.3 ± 5.0	0.549 ± 0.034
B3	5.82 ± 0.02	354.6 ± 1.4	0.504 ± 0.023
B4	6.18 ± 0.18	257.9 ± 4.1	0.493 ± 0.015
B5	6.31 ± 0.10	244.2 ± 1.7	0.516 ± 0.020
B6	6.18 ± 0.03	329.4 ± 8.0	0.562 ± 0.055
B7	6.68 ± 0.08	604.9 ± 11.6	0.758 ± 0.011
B8	6.41 ± 0.04	251.1 ± 6.4	0.500 ± 0.064
B9	6.48 ± 0.04	288.1 ± 6.1	0.473 ± 0.042

Droplet size and polydispersity index

Prepared formulations were analyzed for DS and PDI (Table 2). The data show that increasing Carbopol from 0.5 g (B1, 289,4 nm) to 0.75 g (B2, 300 nm) to 1 g (B3, 355nm) increases in droplet size, likely due to the higher viscosity of the continuous phase, which reduces the efficiency of droplet breakup during emulsification. Formulations B4 and B5, containing increased Tween 80 concentrations (1.5 and 2 g, respectively), exhibited smaller DS (258 nm and 244 nm) compared to B1 (1 g, 289 nm). This reduction can be attributed to enhanced interfacial stabilization and improved emulsification efficiency at higher surfactant levels, leading to the formation of smaller droplets.

Increasing the concentration of CA from 2 g (B1) to 3.5 g (B6) caused an increase in DS (329 nm), whereas a further increase to 5 g (B7) resulted in a pronounced increase in DS (605 nm), likely due to the higher CA content increasing the viscosity and rigidity of the emulgel matrix, which can hinder efficient droplet breakup during emulsification [17].

Increasing the IPM content from 5 g (B1, 289 nm) to 7.5 g (B8) led to a decrease in DS (251 nm), likely due to improved droplet breakup facilitated by the low-viscosity oil. However, further increasing the content to 10 g (B9) resulted in a DS (288 nm) similar to that of B1, suggesting that at higher oil concentrations, the fixed amount of emulsifier is insufficient to fully stabilize the increased oil fraction [18], allowing partial coalescence and limiting further droplet size reduction.

Rheological characterization of emulgel formulations

Given the exploratory nature of the rheological assessment, the results are interpreted in terms of relative trends, formulation grouping, and directional changes rather than absolute quantitative differences.

The oscillatory stress amplitude as a function of strain amplitude for the prepared formulations measured at 25 °C and 32 °C is presented in Fig. 1a and 1b, respectively. At both temperatures, all formulations showed comparable shear stress amplitude–strain amplitude profiles, with an approximately linear response up to 10% strain, indicating similar elastic behavior within the linear viscoelastic region. At higher strain amplitudes, stress amplitude increased in a non-linear manner for all formulations, reflecting progressive structural rearrangement under deformation. Based on shear stress amplitude magnitude, the formulations could be consistently grouped at both temperatures, with lower values observed for B1, B4, B5, B8, and B9, and higher values for B2, B3, B6, and B7. Increasing the measurement temperature from 25 °C to 32 °C led to a decrease in stress amplitude for most formulations across the strain amplitude range. At 0.1% strain, stress amplitude decreased for most formulations, except B7, which remained unchanged, indicating greater thermal stability at low deformation. At 10% strain, stress amplitude decreased for most formulations. At 1000% strain, all formulations displayed lower stress amplitude at 32 °C, with the most pronounced decreases observed in B1, B4 and B8. The results indicate that increasing temperature promotes structural softening and enhanced molecular mobility, with the magnitude of the effect dependent on formulation composition.

Increasing Carbopol from B1 (0.5 g) to B2 (0.75 g) and B3 (1 g) progressively increased stress amplitude. Comparing B1, B4, and B5 (constant Carbopol at 0.5%), increasing Tween 80 had a non-linear effect, decreasing stress amplitude from 0.5% to 0.75%, likely due to partial network disruption, whereas further increase to 1% had minimal additional effect. Increasing CA content (B1 vs B6 vs B7) increased stress amplitude, consistent with reinforcement of mechanical strength through a stronger lipid-based structuring network. In contrast, higher IPM reduced stress amplitude, consistent with a plasticizing effect that lowers resistance to deformation, as observed in B1, B8, and B9, which are richer in oil. At 32 °C, the stress profiles were qualitatively similar, with moderately lower stress amplitudes reflecting thermal softening.

The complex viscosity (η^*) curves for all formulations determined are presented in Fig. 2. At 25 °C (Fig. 2a), B9 exhibited the lowest complex viscosities, while B7 showed the highest values. Across all formulations, η^* remained relatively stable up to approximately 1% strain, followed by a moderate decrease up to 10% strain, and a more pronounced strain-softening response (i.e., a reduction in η^* with increasing strain amplitude) up to 1000% strain, consistent with progressive network deformation under large-amplitude oscillatory shear. Increasing Carbopol from 0.5 g (B1) to 0.75 g (B2) and 1 g (B3) progressively increased viscosity at both low and high shear strains, indicating the key role of Carbopol in network strength. Comparing B1, B4, and B5, increasing Tween 80 from 1% to 1.5-2% led to a decrease in viscosity, particularly at low strain amplitudes, indicating that higher surfactant content partially disrupts the polymeric network. Comparing B1, B6, and B7, increasing CA from 2 g to 3.5-5 g increased complex viscosity at both low and high strain amplitudes, consistent with enhanced structural reinforcement. Finally, comparing B1, B8, and B9, increasing IPM from 5 g to 7.5-10 g reduced complex viscosity, reflecting the plasticizing effect of the oil phase, which lowers resistance to deformation. At 32 °C, the overall trends were similar, although viscosity decreased moderately for most formulations, particularly those rich in oil and surfactants, whereas Carbopol and CA-rich formulations retained higher viscosity, reflecting lower temperature sensitivity. Across all formulations, the observed temperature-related viscosity changes were consistent with moderate thermal softening. Rheological characterization within the LVR of semisolid dosage forms provides essential information on

their internal structure, stability, and performance during manufacturing, storage, and use. The LVR parameters, including G'_0, γ_{LVR}, G'_{LVR}, G''_{LVR}, tan δ_{LVR}, τ_{yield}, η^*_{LVR}, η_{yield}, and the minimum and maximum torque values, determined at 25 °C and 32 °C, are summarized in Tables S5 and S6 in the Supplementary Material.

Increasing Carbopol concentration from 0.5 g (B1) to 1.0 g (B3) resulted in a concentration-dependent enhancement of elastic properties. At 25 °C, higher Carbopol levels were associated with increased G'_0 (B1: 66.2 Pa; B3: 107.2 Pa), G''_{LVR} (B1: 19; B3: 28.6 Pa), τ_{yield} (B1:0.7; B3: 1.7 Pa) and η^*_{LVR} (B1: 6843.3, B3: 11006.3 mPa·s), indicating formation of a denser and more cohesive polymeric network. B1, B2, and B3 were characterized with tan δ_{LVR} of 0.3, confirming dominance of elastic behavior despite thermal stress.

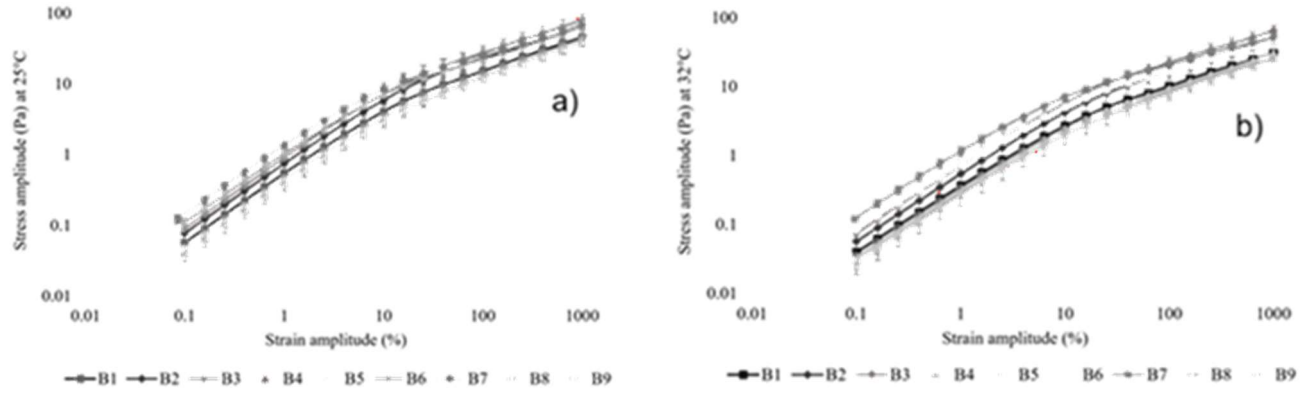

Figure 1. Oscillatory stress amplitude as a function of strain amplitude for the prepared formulations measured at 0 months: a) 25 °C and b) 32 °C. Data are presented as mean ± SD. In cases where SD bars are not visible, the data marker exceeds the size of the error bar.

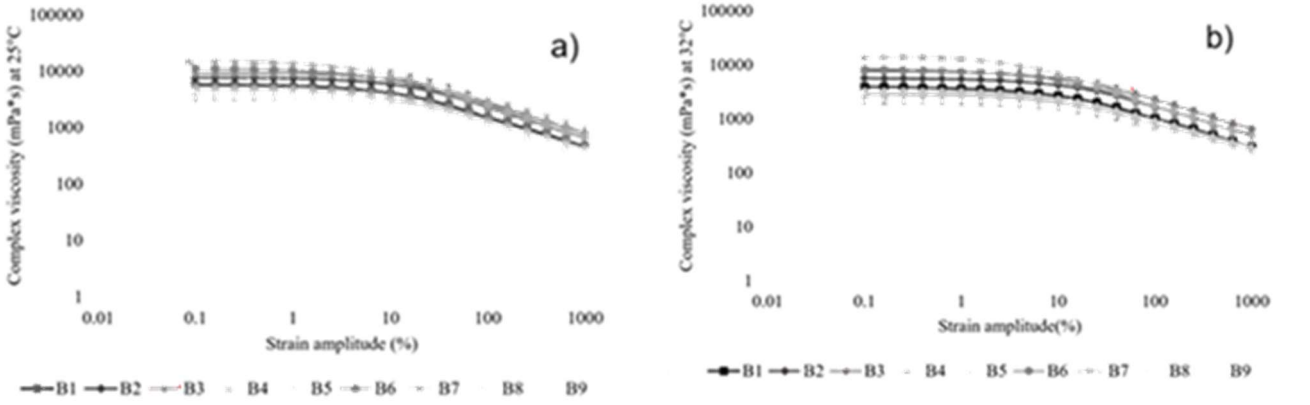

Figure 2. Complex viscosity as a function of strain amplitude for the prepared formulations measured at a) 25 °C and b) 32 °C. Data are presented as mean ± SD. In cases where SD bars are not visible, the data marker exceeds the size of the error bar.

At 32 °C, a temperature-induced decrease in elastic parameters was observed for all 3 samples (e.g., G'_0 decreased from 66.2 Pa to 38.9 Pa for B1, and from 107.2 Pa to 82.3 Pa for B3).

Varying Tween 80 concentration while keeping Carbopol constant (0.5 g) significantly influenced the viscoelastic balance of the emulgels. At 25 °C, increasing Tween 80 from 1.0 g (B1) to 2.0 g (B5) resulted in a reduction of all rheological parameters within the LVR (e.g., G'_0: 66.2 Pa in B1 vs 52.2 Pa in B5 and η^*LVR: 6843.3 mPa·s in B1vs 5545.7 mPa·s in B5), accompanied by an increase in tan δ_{LVR}, indicating a shift toward more viscous-dominated behavior.

Increasing CA content from 2.0 g (B1) to 5.0 g (B7) increases viscoelastic strength. At 25 °C, G'_0 (B1: 66.2; B7: 144.4 Pa), G''_{LVR} (B1: 19; B7: 44.2 Pa), and η^*_{LVR} (B1: 6843.3; B7: 15103.2 mPa·s) increased, reflecting reinforcement of the internal gel structure through a stronger lipid-based network. Although formulations exhibited reduced values at 32 °C, CA-rich formulations (B6 and B7) maintained higher elastic and viscous moduli and yield stress compared to B1 (e.g., G'_0 = 82.1 Pa for B6 and 105.7 Pa for B7 vs 38.9 Pa for B1), demonstrating improved structural integrity at elevated temperature.

Increasing IPM concentration from 5.0 g (B1) to 10.0 g (B9) led to a progressive softening of the emulgel structure. At 25 °C, G'_0 decreased (B1:66.2; B9: 35.8 Pa), with parallel reductions in G''_{LVR} (B1:19; B9: 8.6 Pa) and η^*_{LVR} (B1: 6843.3; B9: 3670.6 mPa·s), indicating dilution and plasticization of the structural network. A similar trend was observed at 32 °C, with overall reductions in viscoelastic parameters compared to 25 °C (G'_0 = 26.5 Pa for B9), consistent with temperature-induced softening. Tan δ values remained low and comparable across formulations (≈0.2-0.3), confirming the predominance of elastic behavior within the linear viscoelastic region despite differences in oil phase content.

Spreadability

The spreadability profiles of all nine formulations (B1-B9) were evaluated over 600 s (Fig. 3). All emulgels showed a rapid initial increase in diameter during the first 60 s, followed by gradual expansion toward a plateau. An intermediate plateau around 120 s was noted with minor increases afterwards up to 600 s, indicating stabilized gel flow under constant load.

All formulations exhibited progressive spreading behavior. While differences in initial diameter and extent of spreading were observed between formulations, the overall profile was comparable across the series. The lowest value corresponds to B5 and B2, and the highest value to B3. These results indicate that all formulations exhibited rapid initial spreading followed by gradual expansion, with B3 showing the highest overall spreadability.

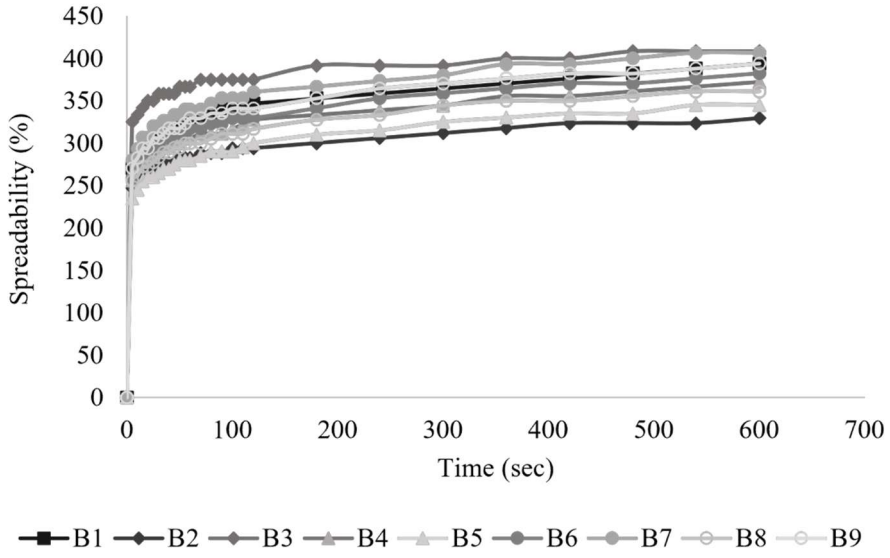

Figure 3. Spreadability curves of the emulgel formulations. The profiles are shown for comparative, early-stage formulation screening.

Drug content assay

The LHCl content in all emulgel formulations ranged from 97.7% to 101.4% of the labeled amount and complied with the predefined CQA acceptance criteria for drug content (95-105%). The minor variations observed among formulations may be attributed to analytical variability, sampling of a semisolid biphasic system, and possible slight water redistribution or evaporation during processing and handling. Nevertheless, all formulations remained within the specified ±5% limits, confirming adequate drug uniformity and content consistency.

In vitro drug release

The dissolution profiles of all formulations are presented in Fig. 4 as cumulative percentage release, while the corresponding mass flux data (mg/cm^2) are shown in Fig. S3. As they are derived from the same experimental dataset obtained under identical conditions (constant membrane diffusion area and LHCl loading), the resulting profiles are directly comparable. However, percentage release was used for the main presentation in accordance with standard pharmaceutical practice to enable straightforward comparison between formulations. This representation was also applied for the calculation of the similarity factor (*f2*) and mean dissolution time (MDT). All samples showed a rapid increase in drug release within the first 30–60 min. At 0.5 h, the percentage of dissolved drug ranged from 6.16% (B9) to 15.61% (B7), indicating pronounced formulation-dependent differences in early release. By 1 h, release values increased to 12.42–22.32%, with B7 again exhibiting the highest release and B9 the lowest. A continuous rise in dissolution was observed up to 6 h, where release ranged between 44.87% (B9) and 72.31% (B7). At the final sampling point (24 h), cumulative drug release varied broadly among formulations, from 57.62% (B9) to 93.50% (B7). In comparison, the LHCl solution showed markedly faster release during the early phase of the experiment, with 32.90% dissolved at 0.5 h, 43.01% at 1 h, and reaching 88.45% by 6 h. At 24 h, cumulative release from the LHCl solution approached 89.93%, demonstrating near-complete dissolution. Overall, formulations B7 and B1 showed the highest release throughout the profile, while B9 exhibited slower dissolution, and the LHCl solution served as a reference for maximal release.

Pairwise comparison of LHCl dissolution profiles was performed using the similarity factor (f_2), and results are summarized in Table S7. The f_2 similarity factor was calculated for exploratory purposes using the available dissolution data and should be considered preliminary. As the full prerequisites for f_2 calculation were not met, dissolution profile similarity was additionally assessed by constructing bootstrap-based confidence intervals for f_2 using 5000 resamples [19], yielding results consistent with the initial f_2 analysis. Formulations were grouped according to the excipient varied to evaluate its effect on drug release. Increasing Carbopol content from 0.5 g (B1) to 0.75 g (B2) and 1 g (B3) resulted in f_2 values >50 for all pairwise comparisons (B1 vs B2, B1 vs B3, B2 vs B3), indicating that

the dissolution profiles remained similar despite the increased polymer content. This confirms that moderate variations in Carbopol primarily modulate the gel network strength without substantially altering the overall release pattern. Increasing Tween 80 concentration from 1% (B1) to 1.5% (B4) resulted in high similarity between B1 and B4, whereas a further increase to 2% (B5) produced dissimilar profiles for both B1 vs B5 and B4 vs B5, indicating that the Tween 80 level can influence the dissolution profile. Increasing CA from 2 g (B1) to 3.5 g (B6) maintained similar dissolution profiles, whereas a further increase to 5 g (B7) resulted in dissimilar profiles for both B1 vs B7 and B6 vs B7, indicating that higher concentrations of the long-chain alcohol can affect the emulsion structure and alter drug release. Increasing the IPM from 5 g (B1) to 7.5 g (B8) maintained similar dissolution (f_2 = 60.66), while further increase to 10 g (B9) led to partial dissimilarity with B1 (f_2 = 49.38) but remained similar with B8 (f_2 = 53.71). These results suggest that moderate oil content does not strongly affect LHCl release, whereas higher concentrations can result in different dissolution profiles. The f_2 analysis indicates that moderate adjustments of formulation components can modulate release rates without dramatically changing dissolution profiles, whereas excessive levels of Tween 80, CA, or IPM can lead to altered release kinetics.

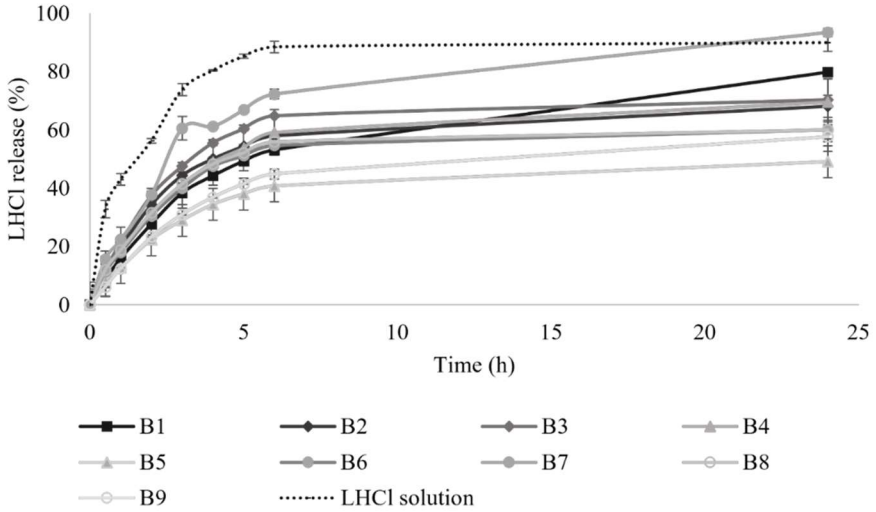

Figure 4. Dissolution profiles of formulations LHCl solution and B1-B9. Data are presented as mean ± SD. In cases where SD bars are not visible, the data marker exceeds the size of the error bar.

MDT (Table S8) was used as an independent parameter to quantify overall drug release rate and assess the effect of formulation composition and storage on release behavior. The LHCl solution showed a very short MDT (1.83 h), confirming rapid drug release from the unstructured system. In contrast, all emulgel formulations (B1-B9) exhibited substantially higher MDT, indicating effective control and prolongation of drug release by the semisolid matrix.

Correlation analysis between formulation, physicochemical, and functional attributes

Correlation analysis revealed clear and consistent relationships between formulation composition, physicochemical properties, rheology, and functional performance over time. At 25 °C (Fig. S1), CA was correlated with pH, DS, and PDI, indicating its strong association with droplet characteristics. CA was also positively correlated with spreadability. In contrast, Tween showed negative correlations with DS, PDI, and spreadability.

All rheological parameters exhibited positive correlations with spreadability, except tan δ_{LVR}. DS and PDI were positively correlated with all rheological parameters, except for tan δ_{LVR} and γ_{LVR}. Under skin-relevant conditions at 32 °C (Fig. S2), rheological parameters remained strongly intercorrelated. DS and PDI were positively correlated with dissolution extents at all sampling points (0.5-24 h) as well as with mean dissolution time (MDT). Dissolution extents were positively correlated with all rheological parameters except tan δ_{LVR} and γ_{LVR}. In addition, dissolution showed positive correlations with Carbopol and CA, and negative correlations with Tween and IPM. MDT exhibited weak positive correlations with DS and PDI and weak negative correlations with most rheo-logical parameters. The strongest correlations with MDT were observed for Carbopol (−0.42) and pH (0.59).

DISCUSSION

The present study applied a QbD framework to systematically develop and characterize LHCl emulgel formulations, with particular emphasis on elucidating the interrelationships between formulation composition, rheology, spreadability, and drug release behavior. The definition of the QTPP and identification of CQAs enabled a structured evaluation of formulation robustness, while correlation analyses supported a mechanistic interpretation of formulation-performance relationships.

All formulations had pH values within the predefined dermal compatibility range (5.0-7.0). The positive correlation between CA concentration and pH likely reflects indirect modulation through microstructural changes and partial shielding of acidic Carbopol groups within a more

structured lipid-polymer network, as previously described for self-bodying semisolid emulsions [20]. DS and PDI data further demonstrated that excipient balance plays a decisive role in emulsion stability. Increasing Carbopol concentration resulted in larger DS, most likely due to elevated continuous-phase viscosity limiting efficient droplet breakup during homogenization, in agreement with classical emulsion theory [21]. In contrast, increasing Tween 80 concentration led to a consistent reduction in DS and improved homogeneity. This observation aligns well with reports by [22], who demonstrated a logarithmic decrease in median DS with increasing nonionic surfactant concentration until saturation of the interfacial area is reached, highlighting the role of surfactant availability in improving interfacial coverage and droplet disruption efficiency during emulsification. CA exerted a dual and concentration-dependent effect on emulsion structure. Studies on oil-in-water creams have shown that mixed fatty alcohols exhibit a pronounced self-bodying action, increasing viscosity and yield value and forming a rigid, gel-like continuous phase [23]. In the present study, increasing CA content was associated with increased droplet size, suggesting that excessive structuring limits efficient droplet breakup and may promote partial coalescence. These findings are consistent with Barry *et al.* [24], who demonstrated that over-structuring by CA alters emulsion microstructure and rheology, potentially favoring globule growth during processing or storage. In the context of the present formulations, such microstructural rearrangements are reflected in increased droplet size and network rigidity, but remain confined to the dispersed-phase architecture without progression to macroscopic instability. Importantly, all formulations remained physically homogeneous throughout preparation and analysis, with no evidence of phase separation, creaming, or syneresis. IPM, a low-viscosity pharmaceutically accepted ester oil, generally promoted DS reduction at moderate concentrations, consistent with its reported ability to facilitate efficient droplet disruption and fine emulsion formation when combined with adequate surfactant levels [25,26]. However, at higher IPM content (10 g), droplet size increased again, indicating that a fixed Tween 80 level became insufficient to stabilize the enlarged interfacial area. This behavior agrees with established emulsion principles and prior studies showing that excessive oil volume fractions without proportional surfactant adjustment predispose systems to partial coalescence and droplet aggregation [27,28].

Rheological parameters derived from amplitude sweep measurements provide essential information on the internal structure, mechanical strength, and in-use performance of emulgels intended for topical application. LVR defines the range of deformation over which the formulation maintains its structural integrity, reflecting resistance to mechanical stresses encountered during storage, handling, and application. Rheological characterization was performed at both 25 °C and 32 °C to capture formulation behavior under laboratory handling and conditions relevant to skin application [29].

Correlation analysis identified Carbopol as the primary determinant of yield stress, strain tolerance (γ_{LVR}), and torque. Strong positive correlations with γ_{LVR} and τ_{yield} indicated enhanced resistance to structural breakdown, while moderate correlations with torque_max reflected formulation rigidity. Associations with viscoelastic moduli and viscosity were weaker than for CA, suggesting Carbopol mainly governs network continuity and yield behavior. CA was a key contributor to elastic strength, viscosity, and microstructural organization across both temperatures. Strong, persistent positive correlations with G_0, G'_{LVR}, G''_{LVR}, η_{LVR}, η_{yield}, and torque demonstrate its role in reinforcing the emulgel matrix. As a long-chain fatty alcohol, CA is known to form semi-crystalline lamellar gel phases in surfactant-water systems, which act as physical crosslinks and enhance network rigidity in semisolid oil-in-water formulations [30]. CA also correlated with droplet size and PDI, indicating promotion of larger, structured dispersed domains that enhance bulk rheological strength. These correlations remained robust at 32 °C, highlighting the thermal stability of the CA-stabilized network. Tween 80 exhibited negative correlations with viscoelastic moduli, viscosity, yield stress, and torque, while positively correlating with tan δ, reflecting a plasticizing effect that enhances molecular mobility and viscous dissipation. IPM showed stronger softening behavior, with negative correlations to G', G'', η, and torque, and positive associations with γ_{LVR} and dissolution at 32 °C. As a low-viscosity oil, IPM facilitates droplet deformation and flow initiation, reducing mechanical strength while promoting drug release, particularly under thermally stressed conditions [31].

Spreadability showed a weak-to-moderate positive correlation with Carbopol content, indicating that within the studied range Carbopol contributed to a structured yet deformable gel network that allowed efficient spreading under applied stress. This behavior is consistent with the shear-thinning properties of Carbopol-based systems reported in topical formulations [32]. Tween 80 exhibited a negative correlation with spreadability. Higher surfactant levels likely enhanced interfacial structuring and internal cohesion of the emulgel, increasing resistance to flow during spreading, as previously described for non-ionic surfactants in semisolid systems [33]. In contrast, CA showed a clear positive correlation with spreadability. As a fatty alcohol and consistency agent, CA promotes lamellar phase formation and internal slip planes, facilitating deformation and improved spreading without compromising structural stability [20,27]. The effect of IPM on spreadability was weaker, with minimal positive correlations.

Spreadability correlated positively with τ_{yield} and γ_{LVR} and negatively with tan δ_{LVR}, indicating formulations with elastic dominance spread uniformly. While amplitude sweep yield stress (Y3) has been reported to correlate with spreadability in semisolid formulations, the direction of correlation depends on the specific spreadability parameter definition. In this study, direct measurement of % spread via the parallel-plate method revealed positive correlations with τyield and G', confirming that elastic-dominant networks promote more efficient spreading. These findings are conceptually in line with previously reported amplitude

sweep correlations with parallel-plate and texture analyzer measurements in semisolid systems [9]. This behavior may be explained by the method-dependent nature of spreadability assessment under parallel-plate compression conditions, where the measured percentage spread reflects structural deformation under applied load rather than purely flow-driven behavior [9,34]. In such systems, deformation occurs through controlled rearrangement of the internal viscoelastic network rather than complete structural breakdown, consistent with the structure-dependent deformation behavior of semisolid topical formulations [6]. Accordingly, spreadability should be interpreted as a composite response governed by both elastic resistance and structural adaptability of the formulation.

All formulations were characterized with LHCl content within acceptance limits. Minor fluctuations were attributed to inherent sampling variability in biphasic semisolid, consistent with previous reports for topical formulations [35]. These findings further support the suitability of the selected excipient systems and processing conditions.

In vitro dissolution studies revealed formulation-dependent differences in LHCl release. While Carbopol concentration modulated gel strength, overall release profiles remained similar within the investigated range, as confirmed by similarity factor analysis. In contrast, variations in Tween 80, CA, and IPM content significantly influenced dissolution kinetics. Correlation analysis highlighted those rheological properties that strongly influenced dissolution behavior. Formulations with higher yield stress (τ_{yield}), larger LVR strain (γ_{LVR}), and greater torque resistance exhibited slower MDT, reflecting the role of gel network strength and resistance to deformation in modulating drug release. Similarly, higher viscoelastic moduli (G'_{LVR}, G''_{LVR}, G_0) and viscosity parameters (η_{LVR}, η_{yield}) determined at 32 °C were generally associated with reduced early dissolution rates (Diss0.5-Diss3), indicating that more cohesive and elastic matrices limit initial drug diffusion [6,36]. Slower release from oil-rich or excessively structured systems and faster release from optimally balanced formulations are consistent with controlled release mechanisms in semisolid matrices, where both network density and drug-excipient interactions govern release rates [37].

CONCLUSION

This study applied an early-stage QbD approach to the development and preliminary characterization of LHCl emulgel formulations. Using a systematic screening of key formulation variables, including Carbopol, Tween 80, CA, and IPM, their influence on CQAs was explored.

Physicochemical characterization indicated that excipient composition dictated droplet size, polydispersity, and in vitro dissolution behavior, with Carbopol and CA enhancing network cohesion and mechanical resistance, Tween 80 modulating interfacial stability, and IPM acting as a plasticizer. Rheological measurements and spreadability assessments, performed as exploratory studies, provided qualitative insights into formulation structure, elastic dominance, and application performance. Correlation analyses highlighted the role of viscoelastic properties and network cohesion in modulating LHCl diffusion.

Overall, the study demonstrates that LHCl emulgels can be rationally designed using a QbD framework, with early-stage exploratory evaluation providing critical information for formulation optimization. The findings emphasize the importance of balancing gelling agents, surfactants, and oil content to achieve formulations that combine chemical stability, desirable rheology, consistent spreadability, and controlled drug release, providing a foundation for further development and long-term stability studies.

REFERENCES

[1] Ajazuddin, A. Alexander, A. Khichariya, S. Gupta, R.J. Patel, T.K. Giri, D.K. Tripathi, J. Controlled Release 171 (2013) 122-132. https://doi.org/10.1016/j.jconrel.2013.06.030.
[2] A.M. Shabery, R.T. Widodo, Z. Chik, Gels 9 (2023) 96. https://doi.org/10.3390/gels9020096.
[3] A. Owsley, R. Misra, A. Awe, J. Ma, G. Verma, A.T. Velaoras, P. Glenn, K. Frasier, Dermis 5 (2025) 1-13. https://doi.org/10.35702/Derm.10030.
[4] P.G. Karamkar, A. Agrawal, V.K. Chatap, Adv. Pharmacol. Pharm. 11 (2023) 90-101. https://doi.org/10.13189/app.2023.110202.
[5] C.V. Pawar, N.V. Pote, M.M. Mule, R.B. Chougale, R.R. Wale, Int. J. Pharm. Sci. 2 (2024) 602-609. https://doi.org/10.5281/ZENODO.11582581.
[6] K. Welin-Berger, J.A.M. Neelissen, B. Bergenståhl, Eur. J. Pharm. Sci. 13 (2001) 309-318. https://doi.org/10.1016/S0928-0987(01)00118-X.
[7] ICH Q8 (R2), Pharmaceutical development - Scientific guideline (2017). https://www.ema.europa.eu/en/ich-q8-r2-pharmaceutical-development-scientific-guideline (accessed January 25, 2026).
[8] S.D. Dutta, J. Bin, K. Ganguly, D.K. Patel, K.T. Lim, RSC Adv. 11 (2021) 20342-20354. https://doi.org/10.1039/D1RA01143J.
[9] E.Y. Al-Barghouthy, S. Hamed, G.F. Mehyar, H.S. AlKhatib, Gels 11 (2025) 1006. https://doi.org/10.3390/gels11121006.
[10] M. Dabbaghi, S. Namjoshi, B. Panchal, J.E. Grice, S. Prakash, M.S. Roberts, Y. Mohammed, Pharmaceutics 13 (2021) 1351. https://doi.org/10.3390/pharmaceutics13091351.
[11] H. Herrada-Manchón, M.A. Fernández, E. Aguilar, Gels 9 (2023) 517. https://doi.org/10.3390/gels9070517.
[12] I. Dimitrovska, T. Olumceva, E. Markova, M. Kostoska, L. Taneska, M. Petrushevska, V. Makrievski, J. Todorov, D. Shalabalija, L. Mihailova, R. Popeski Dimovski, M. Glavas Dodov, M. Simonoska Crcarevska, Cellulose 27 (2020) 7109-7126. https://doi.org/10.1007/s10570-020-03283-7.
[13] J. Sehajpal, J.N. Fairchild, T. Swann, USP Method Modernization for Lidocaine Formulations Using XBridge Columns and Different LC Systems (2018). https://www.waters.com/nextgen/us/en/library/application-notes/2018/usp-method-modernization-for-lidocaine-

formulations.html?srsltid=AfmBOooC-Z5oZSS5z5H3d2qEh319i_2jxniR4kLOFeSaGnaP_5ehKHGA (accessed January 25, 2026).
[14] ICH Q2(R2), Validation of analytical procedures - Scientific guideline (2023). https://www.ema.europa.eu/en/ich-q2r2-validation-analytical-procedures-scientific-guideline (accessed January 25, 2026).
[15] Y. Zhang, M. Huo, J. Zhou, A. Zou, W. Li, C. Yao, S. Xie, AAPS J. 12 (2010) 263-271. https://doi.org/10.1208/s12248-010-9185-1.
[16] Ph. Eur. 11.0, European Pharmacopoeia, EDQM, Strasbourg, (2023). https://www.edqm.eu/en/european-pharmacopoeia.
[17] N.S. Abdelmalak, S.F. El-Menshawe, Int. J. Pharm. Pharm. Sci. 4 (2012) 460-468. https://www.researchgate.net/publication/256457466_A_new_topical_fluconazole_microsponge_loaded_hydrogel_Preparation_and_characterization.
[18] Y. Tian, Y. Guo, W. Zhang, J. Dispersion Sci. Technol. 37 (2016) 1115-1122. https://doi.org/10.1080/01932691.2015.1083440.
[19] J. Muselík, A. Komersová, K. Kubová, K. Matzick, B. Skalická, Pharmaceutics 13 (2021) 1703. https://doi.org/10.3390/pharmaceutics13101703.
[20] B.W. Barry, Dermatological formulations: percutaneous absorption, Dekker, New York, (1983).
[21] D.J. McClements, in Food Emulsions: Principles, Practices, and Techniques, 3rd Edition, Editor Ed., CRC Press, Boca Raton (2015), p. 245. https://doi.org/10.1201/b18868.
[22] M. Artiga-Artigas, J. Montoliu-Boneu, L. Salvia-Trujillo, O. Martín-Belloso, Colloids Surf., A 578 (2019) 123577. https://doi.org/10.1016/j.colsurfa.2019.123577.
[23] S. Fukushima, M. Takahashi, M. Yamaguchi, J. Colloid Interface Sci. 57 (1976) 201-206. https://doi.org/10.1016/0021-9797(76)90193-4.
[24] B.W. Barry, G.M. Saunders, J. Colloid Interface Sci. 38 (1972) 616-625. https://doi.org/10.1016/0021-9797(72)90397-9.
[25] V. Juškaitė, K. Ramanauskienė, V. Briedis, Evidence-Based Complementary Altern. Med. 2015 (2015) 540916. https://doi.org/10.1155/2015/540916.
[26] J. Malakar, S.O. Sen, A.K. Nayak, K.K. Sen, ISRN Pharmaceutics 2011 (2011) 780150. https://doi.org/10.5402/2011/780150.
[27] T.F. Tadros, in Emulsion Formation and Stability, T.F. Tadros Ed., Wiley (2013). p.1 https://doi.org/10.1002/9783527647941.ch1.
[28] G. Urbina-Villalba, Int. J. Mol. Sci. 10 (2009) 761-804. https://doi.org/10.3390/ijms10030761.
[29] A. Mancuso, A. Silletta, M. Verdiglione, N. d'Avanzo, A. Barone, J. Sacco, M.C. Cristiano, D. Paolino, Cosmetics 12 (2025) 239. https://doi.org/10.3390/cosmetics12060239.
[30] H.H. Tran, T.H. Nguyen, T.T. Tran, H.D. Vu, H.M.T. Nguyen, Structures, ACS Omega 6 (2021) 20975-20983. https://doi.org/10.1021/acsomega.1c02439.
[31] C. Zhao, P. Quan, C. Liu, Q. Li, L. Fang, Acta Pharm. Sin. B 6 (2016) 623-628. https://doi.org/10.1016/j.apsb.2016.05.012.
[32] M. Kolman, C. Smith, D. Chakrabarty, S. Amin, Int. J. Cosmet. Sci. 43 (2021) 748-763. https://doi.org/10.1111/ics.12750.
[33] R.J.S. Blount, Md.J. Ferdaus, R.C.D. Silva, Appl. Food Res. 5 (2025) 100796. https://doi.org/10.1016/j.afres.2025.100796.
[34] R. Kryscio, P.M. Sathe, R. Lionberger, L. Yu, M.A. Bell, M. Jay, J.Z. Hilt, AAPS PharmSciTech 9 (2008) 84-86. https://doi.org/10.1208/s12249-007-9009-5.
[35] T. Ilić, I. Pantelić, S. Savić, Pharmaceutics 13 (2021) 710. https://doi.org/10.3390/pharmaceutics13050710.
[36] A.Z.M. Badruddoza, M.I. Zahid, T. Walsh, J. Shah, D. Gates, T. Yeoh, M. Nurunnabi, Int. J. Pharm. 658 (2024) 124210. https://doi.org/10.1016/j.ijpharm.2024.124210.
[37] I. Eros, E.Y. Abu-Eida, I. Csóka, Z. Sánta, A. Cserne, T. Kövér, Drug Dev. Res. 59 (2003) 316-325. https://doi.org/10.1002/ddr.10213.

PRELIMINARNA STUDIJA EMULGELOVA LIDOKAIN-HIDROHLORIDA PRIMENOM PRISTUPA „KVALITET KROZ DIZAJN“

MAJA DJEPANOVA

BILJANA STEFANOVSKA

ANGELA NASTEVSKA

TEODORA TASEVSKA

LINA LIVRINSKA TRPEVSKA

KATERINA GORACINOVA

NIKOLA GESKOVSKI

MAJA SIMONOSKA CRCAREVSKA

Faculty of Pharmacy, Ss. Cyril & Methodius University in Skopje, Republic of North Macedonia

Sprovedeno je rano fazno skrining ispitivanje, zasnovano na pristupu kvalitet kroz dizajn/upravljanje rizikom kvaliteta, za 4% emulgelove lidokain-hidrohlorida (LHCl) tipa ulje u vodi, namenjene za topikalnu primenu. Definisan je ciljni profil kvaliteta proizvoda, kao i kritična svojstva kvaliteta, radi obezbeđivanja efikasnosti, bezbednosti i prihvatljivosti za pacijente. Razvijeno je devet formulacija (B1-B9) kako bi se procenio uticaj ključnih kritičnih svojstava materijala, odnosno Carbopola 940, Tweena 80, cetostearil-alkohola (CA) i izopropil-miristata (IPM), na fizičko-hemijska svojstva, reološko ponašanje, razmazivost i in vitro oslobađanje leka. Sve formulacije pokazale su prihvatljive vrednosti pH, homogenost i sadržaj leka. Veličina kapljica i polidisperznost snažno su zavisile od sastava ekscipijenasa: veći sadržaj Carbopola i CA povećavao je veličinu kapljica, dok ju je Tween 80 smanjivao. Merenja amplitudnog pretraživanja pokazala su ponašanje u kojem dominira elastična komponenta u okviru linearnog viskoelastičnog područja; Carbopol i CA povećavali su viskoelastičnu čvrstoću i napon tečenja, dok su Tween 80 i IPM pokazivali plastifikujući efekat. Razmazivost je bila uporediva među formulacijama i odražavala je ponašanje razređivanja pri smicanju. In vitro ispitivanje rastvaranja pokazalo je da oslobađanje LHCl zavisi od formulacije, pri čemu su jače gel-mreže bile povezane sa sporijim oslobađanjem. Korelaciona analiza potvrdila je značajne odnose između sa-držaja CA, reoloških parametara, veličine kapljica i oslobađanja leka. U celini, emulgelovi LHCl mogu se racionalno dizajnirati primenom pristupa kvalitet kroz dizajn (QbD), pri čemu reološka svojstva i veličina kapljica predstavljaju ključne determinante njihovih performansi.

NAUČNI RAD

Ključne reči: kvalitet kroz dizajn, upravljanje rizikom kvaliteta, topikalna dostava leka, formulacija emulgela.